ISSN: 2321-2152

IJMECE

International Journal of modern electronics and communication engineering

E-Mail
editor.ijmece@gmail.com
editor@ijmece.com

www.ijmece.com

ISSN: 2321-2152www.ijmece .com
Vol 10, Issue.2April 2022

Stiffness analysis of a three-pulley, two-universe (PUU) parallel kinematic machine

D Merwin Rajesh[1,] P Sivaseshu [2] C Nagaraju [3], J Suresh Babu[4]

Abstract

The stiffness of a 3-PUU translational parallel kinematic machine is described in this work (PKM). To generate the stiffness matrix for actuators and restrictions as well as leg compliance, a different technique is employed. Rigidity manipulator performance is evaluated using extreme stiffness values and their design ramifications.It's a smart idea to include the 3-PUU PKM's stiffness into the design of its architecture. The stiffness centre and the compliant axis of the PKM may be identified via an eigenscrew decomposition of the PKM's stiffness matrix, providing a physical interpretation of PKM stiffness.Parallel manipulator kinematics and mechanical stiffness

Introduction

Due to their wide range of uses, parallel manipulators have grown in popularity in recent years [1]. In many applications, parallel manipulators with less than six degrees of freedom (DOF) have been widely used because of the intrinsic advantages of parallel mechanisms, as well as extra benefits in terms of manufacturing and operating costs. The end-precision effector's and cutting speed are directly related to the robustness of parallel mechanisms. A parallel kinematic machine's stiffness must be tested and evaluated as early in the design phase as possible (PKM). The idea of translational parallelism was discussed and investigated prior to the 3-PUU mechanism [5–6]. A little amount of research has been done on the system's overall stiffness, despite actuators and legs having their own compliance. The 3-PUU PKM stiffness model established for this work has an effect on the structure's dynamics, which is why PKM in motion is explored.

[1,2,3,4] Asst. Professor,

Department of ME, K. S. R. M College of Engineering(A), Kadapa

ISSN: 2321-2152www.ijmece .com
Vol 10, Issue.2April 2022

Section 1.1 discusses stiffness modelling.

This connection between force and deflection is linear when elastic devices support a rigid body [7], as defined by a 6x6 positive semidefinite matrix that is symmetrical. End-vector effector of compliant deformations is connected to a static external wrench via a 6x6 stiffness matrix to identify parallel manipulators. Six-leg parallel 6-DOF manipulators with pliability of each compliant portion may be utilised to construct a basic stiffness model. It takes a long time to create stiffness maps for manipulators with just two degrees of freedom. The stiffness of a tripod-based PKM may be mimicked via virtual labour [10]. In [11], a parallel manipulator model for CaPaMan was created by using the kinematic and static features of all three legs.

Present methodologies are inadequate to explain the stiffness of manipulators with fewer degrees of freedom of motion. Prior to this work, methods to construct a parallel manipulator's stiffness matrix using an overall Jacobian were suggested [12]. The 6 x 6 matrix of a translational PKM may summarise the stiffness and restrictions of the actuations of a less-DOF parallel manipulator, according to this work.

Stiffness assessment,

The stiffness of a PKM for a specific set of anipulator settings is determined by the workspace design and the direction in which wrenches are applied. An object stiffness model must be built and forecasted when evaluating whether or not the design meets stiffness standards or even performs an ideal design. its Stiffness behaviour of a PKM must be examined in a variety of settings in order to understand it. An extensive set of performance indicators has been developed and is widely used in the scientific literature to assess stiffness in various materials. Sturdiness may be quantified using the stiffness matrices [8,10].

The eigenvalue of the stiffness matrix for the eigenvector in question may also be used to assess stiffness [8,13]. A rigidity limit has been discovered for stiffness matrices with low and high Eigenvalues, according to study. [14] The stiffness matrix's largest-to-smallest eigenvalue ratio may be used to predict stiffness values. The stiffness matrix may be evaluated in a variety of ways, including its determinant, which is the product of its eigenvalues. The stiffness of a three-dof spherical parallel manipulator may be calculated by dividing the workspace volume by the stiffness matrix [15].

ISSN: 2321-2152www.ijmece .com
Vol 10, Issue.2April 2022

The typical form of the stiffness matrix has off-diagonal components, making it impossible to accurately define the stiffness attribute in any direction. Even though the manipulator's poor stiffness precludes it from being employed in applications, the determinant or trace values are quite high because or trace cannot distinguish the difference.

A machine tool must have a minimum stiffness level throughout its workspace, even if the condition number suggests that the stiffness matrix has been incorrectly prepared for consistent manipulation. Since the lowest and highest stiffness values as well as their variations are used to assess performance, this article uses them.

Understanding the spatial compliance of a PKM necessitates using a stiffness model for the PKM. If the stiffness matrix is broken down into its individual eigenscrews, a physical explanation for spatial elastic behaviour may be found. This physical interpretation is possible [18] if the stiffness centre and the compliant axis are present. The RCC (remote centre of compliance) concept may be expanded to incorporate off-diagonal blocks diagonalized at the centre of stiffness in the stiffness matrix specification. It is nevertheless possible for rotation and translation to be separated when the normal form of a generic stiffness matrix is not diagonal. As a torsional and linear spring in one device, it's used in robotics. Both linear and rotational deformation are parallel when applied to the axis of a compliant system. No matter how rigid the system, this is what happens all the time.

3-PUU PKM is introduced in Section 2; a novel approach for computing the stiffness matrix is explained in Section 3. A product's structural integrity may be predicted using shock indices, which are discussed in Section 4. Section 5 wraps things up with a few last thoughts.

Kinematic description

Figure 1 depicts the CAD model of a 3-PUU PKM, whereas Figure 2 shows the schematic design. A movable platform, a stationary base, and three arms with the same kinematic framework make up the manipulator. Lead screw linear actuators are used to drive (U) joints sequentially. Because each U joint is made up of two revolute (R) joints that meet at an angle, each limb may move like a Chain of motion PRRRR. Only translational movements can be achieved using a 3-PUU mechanism.

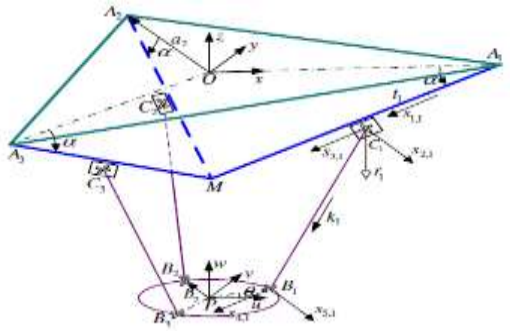

Fig. 2. Schematic representation of a 3-PUU PKM.

For each chain, the initial and last revolute joints are parallel, and the two intermediate joint axes are also parallel. Figure 2 shows the fixed Cartesian reference frame (Ox,y,z) we'll be using for this inquiry. The permanent base of the platform and the movable frame of the mobile platform. Triangle DB1A2B3 and triangle DB1B2B3 intersecting The x and u axes should be aligned to make things easy. OA1 is used to designate the x-axis. Oai and OAi are the vectors' angles to each other PBi "I 1; 2; 3" is a novel way of putting it. Angle h, therefore, is the angle formed by a moving platform and a stationary base. On one of its three tracks, AiM crosses across. The x–y plane has three points where circles of the same radius intersect: A1, A2, and A3, as well as M, where a third circle of the same radius crosses. Circles B1, B2, and B3 are the intersection locations of the three legs CiBi with lengths l in the U–V plane. Its circumference is b Angle an is defined as the angle of motion of the actuators from the base to the rails AiM. Perspective. To guarantee that the manipulator has a symmetric workspace, DA1A2A3 and DB1B2B3 must be used. Equilateral triangles are being distributed. Leg CiBi represents the actuator's linear displacement and its rotation. An indicator of the unit vector should be shown on the AiM rail. Make sure ai gets a quarter of OAi, too One-eighth PBI is an alternative.For every time, there is a four-fold multiplier. Vector-loop analysis may be used to address both forward and backward motion issues. Closed-form solutions may exist. Solutions to inverted kinematics may be summed up as follows:

ISSN: 2321-2152www.ijmece .com
Vol 10, Issue.2April 2022

As a result of this data, the 3-PUU PKM's workspace is now revealed.

$$d_i = \mathbf{k}_i^T \mathbf{e}_i - \sqrt{(\mathbf{k}_i^T \mathbf{e}_i)^2 - \mathbf{e}_i^T \mathbf{e}_i + r^2}, \quad (1)$$

where $\mathbf{e}_i = \mathbf{p} + \mathbf{b}_i - \mathbf{a}_i$ for $i = 1, 2,$ and 3.

Stiffness matrix generation

Jacobian matrix derivation

The Jacobian matrix of a parallel manipulator may be derived using reciprocal screw theory [12]. The mobile platform's twist may be described as T 14 12tT xTT in Plu cker axis coordinates, with t and x designating the vectors for linear and angular velocities, respectively.

$$\$ = \dot{d}_1 \hat{\$}_{1,1} + \dot{\theta}_{1,2} \hat{\$}_{1,2} + \dot{\theta}_{1,3} \hat{\$}_{1,3} + \dot{\theta}_{1,4} \hat{\$}_{1,4} + \dot{\theta}_{1,5} \hat{\$}_{1,5} \quad (2)$$

A unit screw (in Plu cker coordinates) is connected with each of the joints of the leg in which the intensity is equal to or greater than _hj;i, where I is 1, 2, or 3.

$$\hat{\$}_{1,1} = \begin{bmatrix} \mathbf{s}_{1,1} \\ \mathbf{0} \end{bmatrix}, \quad \hat{\$}_{1,2} = \begin{bmatrix} \mathbf{c}_1 \times \mathbf{s}_{1,2} \\ \mathbf{s}_{1,2} \end{bmatrix}, \quad \hat{\$}_{1,3} = \begin{bmatrix} \mathbf{c}_1 \times \mathbf{s}_{1,3} \\ \mathbf{s}_{1,3} \end{bmatrix}, \quad \hat{\$}_{1,4} = \begin{bmatrix} \mathbf{b}_1 \times \mathbf{s}_{1,4} \\ \mathbf{s}_{1,4} \end{bmatrix}, \quad \hat{\$}_{1,5} = \begin{bmatrix} \mathbf{b}_1 \times \mathbf{s}_{1,5} \\ \mathbf{s}_{1,5} \end{bmatrix}$$

The following equations are used to determine sj;i, For the 3-PUU mechanism's joint axis, the translational PKM has to fulfil criteria s3;14, First, a ray coordinate of one screwtc;i, which is reciprocal to all other screwstc;i of the ith joint. Secondly, a ray coordinate A 1-system is a screw with an infinite pitch that is oriented perpendicular to the limb. The articulation of a U-joint is divided into two axes:

$$\hat{\$}_{1,5} = \begin{bmatrix} \mathbf{0} \\ \mathbf{r}_1 \end{bmatrix}, \quad (3)$$

Eq. (2) may be constructed into a matrix form by taking the product of both sides of the equation with tc;i.

$$\mathbf{J}_c \mathbf{T} = \boldsymbol{\theta}, \quad (4)$$

where

$$\mathbf{J}_c = \begin{bmatrix} \mathbf{0} & \mathbf{r}_1^T \\ \mathbf{0} & \mathbf{r}_2^T \\ \mathbf{0} & \mathbf{r}_3^T \end{bmatrix}_{3\times 6} \quad (5)$$

is referred to as the Jacobian principle of constraint. The mobile platform's 3-DOF mobility is restricted by the combination of the limitations in each row of Jc. The unique solution to Eq. (4) if ri is: x 14 0. This system contains the, Screwtc;i had already figured it out. All the passive joint screws of the extra basis screwta;i are reciprocal zero pitch screw may be distinguished along the path of the two U joints, i.e.

$$\hat{\$}_{2,5} = \begin{bmatrix} \mathbf{k}_2 \\ \mathbf{b}_2 \times \mathbf{k}_2 \end{bmatrix}. \quad (6)$$

Similarly, taking the product of both sides of Eq. (2) with $\hat{\$}_{2,5}$, leads to a matrix-form result:

$$\mathbf{J}_a \mathbf{T} = \dot{\mathbf{q}}, \quad (7)$$

where $\dot{\mathbf{q}} = [\dot{d}_1 \ \dot{d}_2 \ \dot{d}_3]^T$ denotes the actuated joint rate and

$$\mathbf{J}_a = \begin{bmatrix} \frac{\mathbf{k}_1^T}{\mathbf{k}_1^T \mathbf{s}_{1,1}} & \frac{(\mathbf{b}_1 \times \mathbf{k}_1)^T}{\mathbf{k}_1^T \mathbf{s}_{1,1}} \\ \frac{\mathbf{k}_2^T}{\mathbf{k}_2^T \mathbf{s}_{2,1}} & \frac{(\mathbf{b}_2 \times \mathbf{k}_2)^T}{\mathbf{k}_2^T \mathbf{s}_{2,1}} \\ \frac{\mathbf{k}_3^T}{\mathbf{k}_3^T \mathbf{s}_{3,1}} & \frac{(\mathbf{b}_3 \times \mathbf{k}_3)^T}{\mathbf{k}_3^T \mathbf{s}_{3,1}} \end{bmatrix}_{3\times 6} \quad (8)$$

it's known as the Jacobian of motions. Ja's units demonstrate following talks. As a result, in order to construct a stiffness matrix, the Jacobian matrix units must be homogenised. Invariant to the length unit selected, the performance index The dimensionally homogenous Jc is dimensionless.It is possible to attain the Jacobian of actuations

$$\mathbf{J}_{ah} = \mathbf{J}_a \mathbf{W} \quad (9)$$

with $\mathbf{W} = \mathrm{diag}[1, 1, 1, \frac{1}{b}, \frac{1}{b}, \frac{1}{b}]$, where the mobile platform radius b is chosen as the characteristic length to homogenize the dimension of the Jacobian matrix.

Combining Eqs. (4) and (7) allows the generation of

$$\dot{\boldsymbol{\phi}}_p = \mathbf{J}\mathbf{T}, \quad (10)$$

where $\dot{\boldsymbol{\phi}}_p = [\dot{d}_1 \ \dot{d}_2 \ \dot{d}_3 \ 0 \ 0 \ 0]^T$ is the extended joint rate, and

$$\mathbf{J} = \begin{bmatrix} \mathbf{J}_{ah} \\ \mathbf{J}_c \end{bmatrix}_{6\times 6} \quad (11)$$

is called the overall Jacobian of a 3-PUU PKM, which is homogeneous in terms of units.

Stiffness modelling is discussed in section

Three constraint couples are exerted on the movable platform by the wrench system that is the reciprocal screw system with infinite pitch and by the reciprocal screw system with zero pitch. Three forces are applied to the movable platform via the screw system of actuation. the limbs. In other words, each leg is subjected to one and a half times its own weight in a certain direction. Considering the premise Infinite rigidity of the U joints and mobile platform and the compliance of actuators and legs are the only constraints may be deduced in this manner.

ISSN: 2321-2152www.ijmece .com
Vol 10, Issue.2April 2022

Control of actuators affects compliance

To move a lead screw, the torque must be transmitted between the ith nut and the linear displacement may be estimated as a function of time

$$f_i = \frac{2\tau_i}{\mu_c d_s} \text{ and } \Delta l_i = \frac{f_{ai}}{K_{ai}}, \quad (12)$$

Assume that lc is the friction coefficient of the ith actuator, si is its torsional stiffness, and ds is its pitch diameter. According to Eq. (12), one can calculate the linear driving device's compliance:

$$C_i = \frac{\Delta l_i}{f_i} = \frac{\mu_c d_s p}{2K_{ai}}. \quad (13)$$

As a result, the projection of compliance in the corresponding leg's direction may be deduced as a function of the it actuator.

$$C^k_{a,i} = \hat{k}_i^T s_{i,i} C_i. \quad (14)$$

Legs-based compliance

Transverse compliance is equal to the ith leg's Ckl;i, whereas longitudinal compliance is the same. There is an elastic deformation of the ith leg because of a constraint force Fki and a constraint couple Mri perpendicular to the limb's universal joint. This means that the elastic deformations may be represented as follows:

$$\Delta l_i = C^k_{l,i} F^k_i = \frac{l}{AE} F^k_i, \quad (15)$$

$$\Delta \theta_i = C^k_{\theta,i} M^r_i = \frac{l}{GI_p} \hat{k}_i^T \tau_i M^r_i, \quad (16)$$

There are two legs, each with a length of l and a cross-sectional area of A, and each leg has a modulus of elasticity E and G, respectively. Eqs. (15) and (16) may then be used to generate Ckl I and Ck h;i.

The stiffness model

Constraints' and actuators' stiffnesses may be calculated using the inverse connection between stiffness and compliance

$$K_{a,i} = C_{a,i}^{-1} = (C^k_{a,i} + C^k_{l,i})^{-1},$$
$$K_{c,i} = C_{c,i}^{-1} = (C^k_{\theta,i})^{-1}$$

for $i = 1$, 2, and 3.

Consider that three linear springs are used to link the movable platform to the stationary base, and three rotating springs are used as well, as shown in Fig.

Stiffness matrix determination

Suppose an external wrench w 14 12fT is applied to the movable platform in the form of the Plu cker ray coordinate, where force is denoted by the notation F 14 12fx, torque is denoted by the notation M 12mx, and so on. The response forces/torques of the actuators and restraints, respectively, may be represented by the sa and sc symbols. Reaction forces/torques exerted by actuators and restraints, i.e., the external wrench is balanced in the absence of gravity

$$w = J_a^T \tau_a + J_c^T \tau_c, \quad (18)$$

where the reaction forces/moments can be expressed as

$$\tau_a = \chi_a \Delta q_a, \quad (19a)$$

$$\tau_c = \chi_c \Delta q_c \quad (19b)$$

the matrices are va 14 diag1–2Ka;1; Ka;2–3 and vc, respectively, which represent the displacements of actuations and restrictions, respectively, in the form of Dqa and Dqc. It is also possible to calculate the displacements of translation and rotation of the movable platform with respect to the three reference axes by using the formula: dx 14 12Dx Dy DzT ; dh 14 12Dhx Dhy DhzT. Then, by ignoring the gravitational impact, the formation of virtual labour is possible.

$$w^T \Delta X = \tau_a^T \Delta q_a + \tau_c^T \Delta q_c, \quad (20)$$

where $\Delta X = [\Delta x^T \ \Delta \theta^T]^T$ denotes the mobile platform's twist deformation in the axis coordinate.

ISSN: 2321-2152www.ijmece .com
Vol 10, Issue.2April 2022

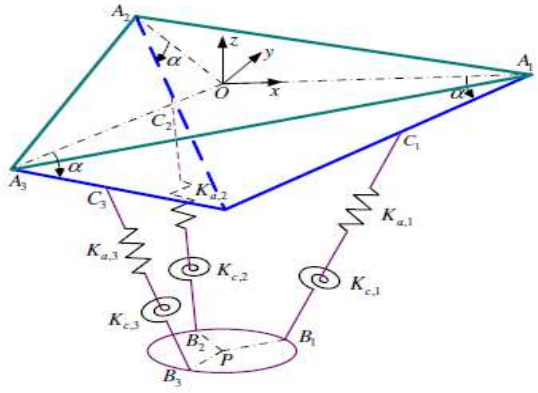

Fig. 3. Stiffness model of a 3-PUU PKM.

A careful analysis of Eqs. (18)–(20) at the same time, leads to the expression of

$$\mathbf{n} = \mathbf{K}\Delta\mathbf{x}, \qquad (21)$$

in where K 14 JTvJ is defined as the 6-by-6 overall stiffness matrix of a 3-PUU PKM, encompassing the influence of actuations and restrictions, with the 6-by-6 diagonal matrix v 14 diag12va vc. Where

Evaluation of the 3-PUU PKM's stiffness

As can be seen in Table 1, the 3-PUU PKM's design parameters aim to strike a balance between the overall workspace's global dexterity index and the space utility ratio index, which measures the workspace's volume in relation to the robot's physical size [6]. In addition, the U joints' cone angle restrictions are 20, and the P joints' motion range limits are D0.1 m. The manipulator's accessible workspace is constructed as illustrated in Fig. 4 using a numerical search approach described in [19]. Moreover, Table 2 details the design's physical properties (3-PUU PKM). Di 14 0 -i 14 1; 2; 3 is the home position of the mobile platform in the case of mid-stroke linear actuators, in which the stiffness matrix is derived as follows:

Table 1
Architectural parameters of a 3-PUU PKM

Parameter	Value
a	0.3 m
b	0.1 m
l	0.3 m
α	45.0°
θ	0.0°

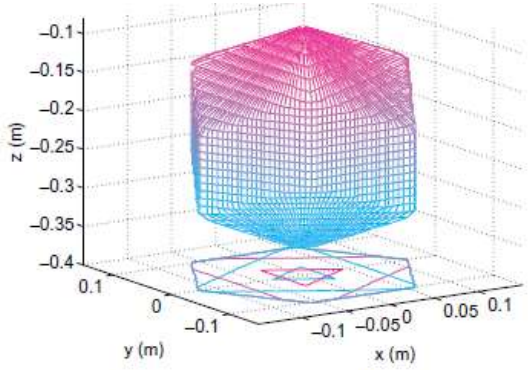

Fig. 4. Reachable workspace of a 3-PUU PKM.

Table 2
Physical parameters of a 3-PUU PKM

Parameter	Value	Parameter	Value
$K_{a,i}$	1.45 x 10^{8} N·m/rad	E	2.03 x 10^{11} N/m^2
k_c	0.25	G	7.85 x 10^{10} N/m^2
d_c	20 mm	A	2.01 x 10^{-4} m^2
t	3 mm	I_y	3.22 x 10^{-8} m^4

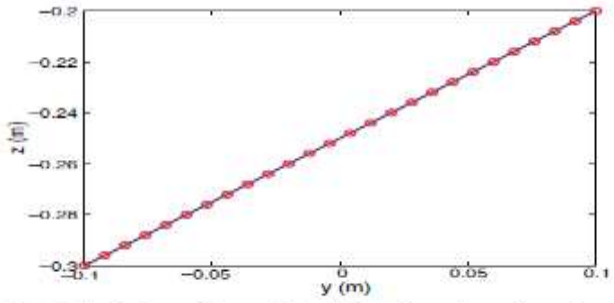

Fig. 5. Trajectory of the mobile platform in a plane of $x = 0$ m.

ISSN: 2321-2152www.ijmece .com
Vol 10, Issue.2April 2022

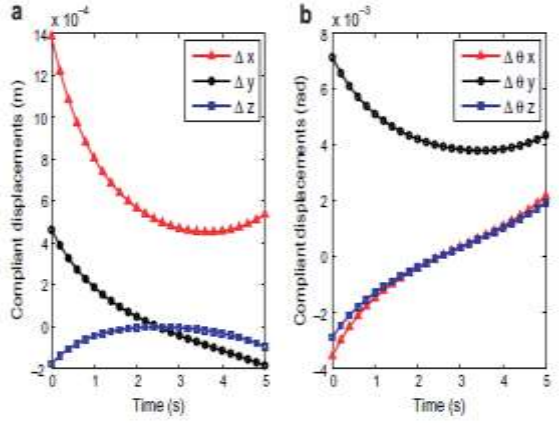

Fig. 6. The compliant displacements of (a) translations and (b) rotations of the mobile platform.

$$K^0 = \begin{bmatrix} 9.0891 & 0 & 0 & 0 & -1.0162 & 0 \\ 0 & 9.0891 & 0 & 1.0162 & 0 & 0 \\ 0 & 0 & 22.7228 & 0 & 0 & 0 \\ 0 & 1.0162 & 0 & 0.1137 & 0 & 0 \\ -1.0162 & 0 & 0 & 0 & 0.1137 & 0 \\ 0 & 0 & 0 & 0 & 0 & 0.0001 \end{bmatrix} \times 10^7,$$

Words N/m are used in this context to describe the phrases K0 11g; K113g; and N/rad to describe the phrases N/mg; K015g; and N/mg. PKM's movable platform may be utilised to calculate the DX's compliant displacement in light of Equation (21). As seen in FIG. 6, the platform moves at a constant speed while being exposed to a static external force of 20 N. It was found that the linear compliant displacement along the x-axis was 1.4 mm, as predicted. In addition to this, the y-axis rotation is the most rotary-compliant displacement of them all.

Stiffness assessment

PKM manipulation demands a stiffer workspace than a predetermined threshold. An overall view of the workspace's stiffness levels may be achieved through determining the lowest and biggest stiffness eigenvalues using classical eigenvalue decomposition. The entire stiffness of the PKM workspace was assessed quantitatively. Volume V division in cartesian coordinates as well as an appraisal of individual parts to identify whether or not they belong in the workspace are essential components of this technique. The size of the samples needed depends on the degree of accuracy. Mechanical joint motion limitations and inverse kinematic solutions are employed for verification. Decomposition of a stiffness matrix produces the components that fall within a specific workspace's limits. For each sample, the lowest and largest stiffness values are compared to establish the workspace's minimum and maximum stiffness values. It has been adopted because it is straightforward to apply in a computer code. [20] A Gough-type parallel manipulator may benefit from a computer round-off analysis approach. It may also be used to create and compare two 3-DOF PKMs [3].

Figure 7 depicts the stiffness levels in the z = 0.242 m (home position height) planes. There are three P joints with 120 degree x–y rotations in the viewing workspace, as depicted. In addition, a manipulator's minimum stiffness and maximum stiffness rise as it approaches the workspace boundary. When deployed outside of the achievable workspace, the PKM exhibits poor stiffness properties. It makes logical to keep it there. This subworkspace's definition is governed by the PKM tasks and performance indicators. Workspace is split into a cubic shape with a 0.01 m edge length, with the platform's home location given as the middle. " Stiffness is studied by modifying the kinematic parameters. As small as 0.002 mm in diameter, the stiffness of this workspace may be determined. In Figs. 8a–d, the 3-PUU PKM's stiffness fluctuates slightly, which is consistent with the 3-PUU PKM's design parameters.

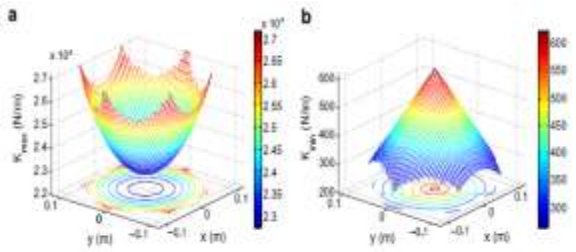

Fig. 7. The distribution for (a) minimum and (b) maximum stiffness in a plane of z = −0.224 m.

ISSN: 2321-2152www.ijmece .com
Vol 10, Issue.2April 2022

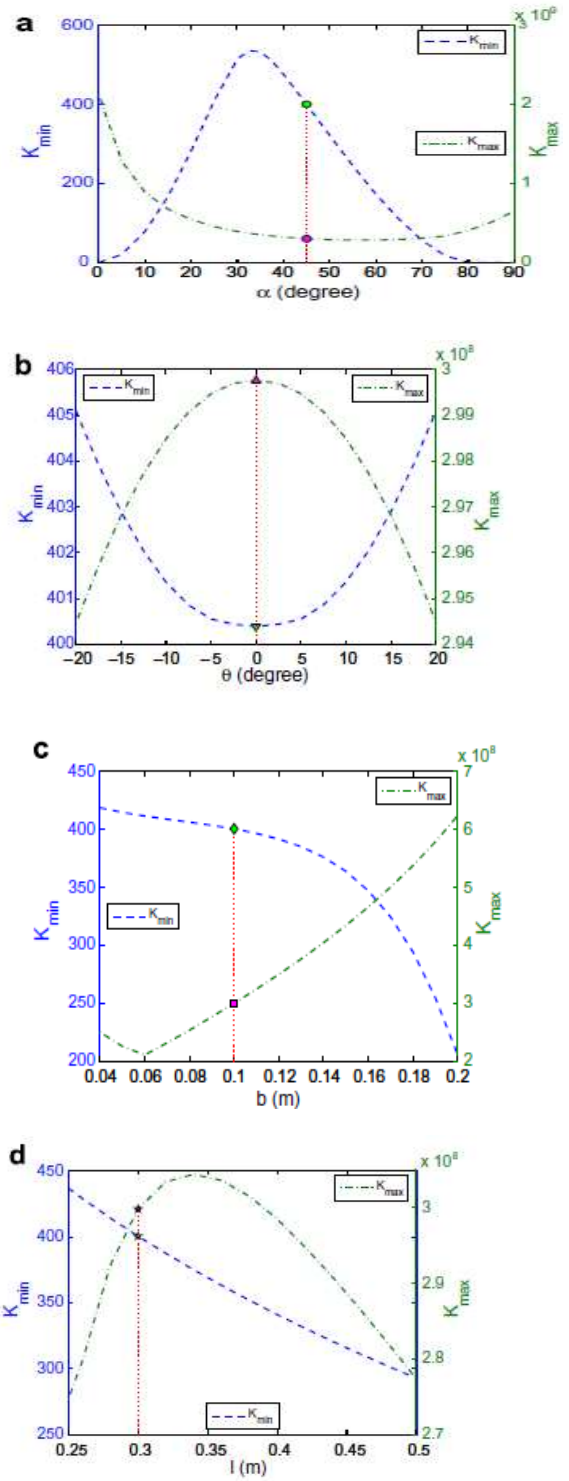

Fig. 8. Global stiffness index versus design parameters of (a) actuators layout angle, (b) twist angle, (c) mobile platform size, and (d) the leg length.

The manipulator's rigidity must be taken into consideration. Between 0 and 90 degrees, the minimum stiffness seems to peak between 30 and 35 degrees, while the maximum stiffness seems to reach its lowest value at 60 degrees. Minimum and maximum stiffness values are lowest for twist angles of h 14 0 as the movable platform size goes from 0.25 metres to 0.50 metres, but maximum stiffness is largest for these twist angles. These twist angles have the lowest minimum and maximum stiffness values. To observe the stiffness of the manipulator at different locations, look at Figure 8. This figure illustrates that the maximum minimum stiffness standards for dexterity and workplace performance are not met, as illustrated. Depending on the activities to be done, stiffness indices may be utilised to examine how well the PKM's architecture optimization is functioning for machine tool applications.

Stiffness interpretation via eigenscrew decomposition

To discover out how stiff the structure is, we'll do an eigenscrew matrix decomposition. Twists are represented in the axis coordinate system, while wrenches are represented in the ray coordinate system. If you want to acquire useful results from the stiffness matrix eigenscrew problem, you must construct it consistently. Some scenarios necessitate the usage of ray or axis screw-based coordinates. It also insures that the results are not depending on the coordinate frame and that the units are preserved as they should be. The results won't hold up without this step, so it's of no practical relevance. The bD matrix may be used to transition between two separate kinds of coordinate systems.

ISSN: 2321-2152www.ijmece .com
Vol 10, Issue.2April 2022

Table 3
Spring constant and geometrical connection for each screw spring

Spring	$k \times 10^{-4}$	$\mathbf{n}^T$	$\mathbf{r}^T$	p
s_1	1.1361	[0, 0, 1]	[0, 0, 0]	−0.0148
s_2	1.1361	[0, 0, 1]	[0, 0, 0]	0.0148
s_3	0.4545	[0.8001, 0.4749, 0]	[0, 0, −0.1111]	−0.0166
s_4	0.4545	[−0.0262, −0.5624, 0]	[0, 0, −0.1111]	0.0166
s_5	0.4545	[−0.0256, −0.9997, 0]	[0, 0, −0.1111]	−0.0166
s_6	0.4545	[−0.0247, −0.9997, 0]	[0, 0, −0.1111]	0.0166

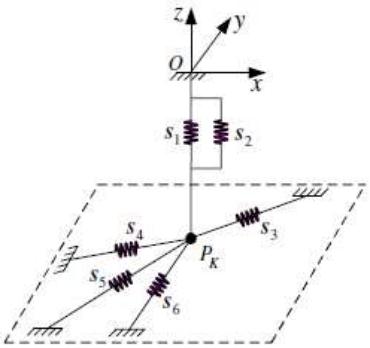

Fig. 9. The physical interpretation of the stiffness of a 3-PUU PKM.

In terms of relevance, the number 2 is important. Therefore, the spring constant k, the helical joint pitch p, and the geometrical connection parameters n and r define the spring properties of each screw spring. No doubt, the first two springs are perpendicular to one another and in the same plane as one another, while the last four are perpendicular to one another and in the "z-plane. " The centre of stiffness, where rotations and translations may be decoupled to the maximum degree feasible, is represented by six springs linked at a single point.

Compliant axis determination

[18] In order to produce a compliant axis, the linear deformation must be parallel to the rotational deformation surrounding it. Only a compliant axis can address the eigenscrew issue. There must be two collinear screws with equal stiffness and opposing signs in order for a compliant shaft to operate. The two collinear eigenscrews define the compliant axis.

Conclusions

The reciprocal screw theory, which accounts for the effects of actuation and restriction on a Jacobian overall, is employed in its design. Additionally, a model of the manipulator's stiffness is constructed that contains both actuators and legs. PKM stiffness may be assessed using the lowest and largest eigenvalues of the stiffness matrix in a cubic form useful workspace. This paper addresses design concerns that effect the stiffness of a building's 3-PUU PKM. Deconstructing the stiffness matrix using eigenscrews is the best technique to understand the PKM's compliant behaviour. Stiffness may be tested by hanging a body from a set of screw springs in a specified manner. Since the PKM's rigidity centre and compliant axis always point in the same direction, it has a greater z-axis stiffness. We have achieved considerable progress in our understanding of 3-PUU PKM stiffness modelling, the evaluation of PKM stiffness using architectural parameters, and a physical interpretation of PKM stiffness. Further parallel manipulators may be simulated using the analytical approaches presented here. The stiffness attributes of the 3-PUU PKM may be utilised as a starting point for architectural design. An experiment is required to validate the results of the stiffness research after the PKM is constructed and manufactured.

References

[1] J.-P. Merlet, Parallel Robots, Kluwer Academic Publishers, London, 2000.

[2] M. Carricato, V. Parenti-Castelli, A family of 3-DOF translational parallel manipulators, ASME J. Mech. Des. 125 (2) (2003) 302–307.

[3] D. Chablat, P. Wenger, F. Majou, J.-P. Merlet, An interval analysis based study for the design and the comparison of three-degreesof-freedom parallel kinematic machines, Int. J. Robot. Res. 23 (6) (2004) 615–624.

[4] Y. Li, Q. Xu, Kinematic analysis and design of a new 3-DOF translational parallel manipulator, ASME J. Mech. Des. 128 (4) (2006)729–737.

[5] L.W. Tsai, S. Joshi, Kinematics analysis of 3-DOF position mechanisms for use in hybrid kinematic machines, ASME J. Mech. Des.124 (2) (2002) 245–253.

[6] Y. Li, Q. Xu, A new approach to the architecture optimization of a general 3-PUU translational parallel manipulator, J. Intell.Robot. Syst. 46 (1) (2006) 59–72.

[7] S. Huang, J.M. Schimmels, Minimal realizations of spatial stiffnesses with parallel or serial mechanisms having concurrent axes,J. Robot. Syst. 18 (3) (2001) 135–146.

[8] C. Gosselin, Stiffness mapping for parallel manipulators, IEEE Trans. Robot. Automat. 6 (3) (1990) 377–382.

[9] N. Simaan, M. Shoham, Stiffness synthesis of a variable geometry six-degrees-of-freedom double planar parallel robot, Int. J. Robot.Res. 22 (9) (2003) 757–775.
[10] T. Huang, X. Zhao, D.J. Whitehouse, Stiffness estimation of a tripod-based parallel kinematic machine, IEEE Trans. Robot. Automat. 18 (1) (2002) 50–58.
[11] M. Ceccarelli, G. Carbone, A stiffness analysis for CaPaMan (Cassino Parallel Manipulator), Mech. Mach. Theory 37 (5) (2002) 427–439.
[12] S.A. Joshi, L.W. Tsai, Jacobian analysis of limited-DOF parallel manipulators, ASME J. Mech. Des. 124 (2) (2002) 254–258.
[13] S. Bhattacharyya, H. Hatwal, A. Ghosh, On the optimum design of Stewart platform type parallel manipulators, Robotica 13 (2)(1995) 133–140.
[14] B.S. El-Khasawneh, P.M. Ferreira, Computation of stiffness and stiffness bounds for parallel link manipulators, Int. J. Mach. ToolsManuf. 39 (2) (1999) 321–342.
[15] X.-J. Liu, Z.-L. Jin, F. Gao, Optimum design of 3-DOF spherical parallel manipulators with respect to the conditioning and stiffnessindices, Mech. Mach. Theory 35 (9) (2000) 1257–1267.
[16] H. Lipkin, J. Duffy, Hybrid twist and wrench control for a robotic manipulator, ASME J. Mech. Transm. Autom. Des. 110 (1988)138–144.
[17] S. Huang, J.M. Schimmels, The eigenscrew decomposition of spatial stiffness matrix, IEEE Trans. Robot. Autom. 16 (2) (2000) 146–156.
[18] T. Patterson, H. Lipkin, A classification of robot compliance, ASME J. Mech. Des. 115 (3) (1993) 581–584.
[19] Y. Li, Q. Xu, Kinematics and stiffness analysis for a general 3-PRS spatial parallel mechanism, in: Proceedings of 15th CISMIFToMMSymposium on Robot Design, Dynamics and Control, 2004, Rom04-15.
[20] J.-P. Merlet, Solving the forward kinematics of a Gough-type parallel manipulator with interval analysis, Int. J. Robot. Res. 23 (3)(2004) 221–235.